New wall law treatment for the Large Eddy Simulation of turbulent heat transfer in a periodic channel ($\mathrm{Re}_\tau = 590$)

1 Introduction

Validation made by : Pierre-Emmanuel Angeli.
Report generated 28/10/2013.

1.1 Description

• Turbulent channel flow.
• Validated model: Robin boundary condition at walls for L.E.S. with wall function in VEF discretization.
• Validation with the analytical law of Reichardt [1]: $U^+ = R(y^+)$, and with the DNS of Moser-Kim-Mansour [2].

1.2 Parameters Trio_U

- Version Trio_U : 1.6.7 ;
- Version Trio_U from out: /work/trioform/PEA/Baltik_Pironneau/basic_opt (1.6.7)
- Type of problem: hydraulics ;
- Discretizations: `VDF` and `VEFPreP1B` ;
- Equations: `Navier_Stokes_turbulent` ;
- Turbulence model: Large Eddy Simulation ;
- Modeling of sub-filter scales: `sous_maille_WALE` (Wall-Adapting Local Eddy-viscosity [3]) ;
- Wall functions: `loi_standard_hydr` ;
- Type of boundary conditions: periodicity in x and z directions, wall for top/low boundaries ;
- Time schemes: `Runge_Kutta_ordre_3` with `facsec` = 1 ;
- Convection schemes: `centre` (velocity) for VDF simulations ; `EF_stab` for VEF simulations.

1.3 Test cases

- T0Q_VDF/Cas.data :
- T0Q_VEF/Cas.data : */*jdd en annexe*/*
- T0Q_VEF_Pironneau/Cas.data : */*jdd en annexe*/*
- T0Q_VEF_Pironneau_maillage_decale/Cas.data :

1.4 References :

- [1] J. O. Hinze, *Turbulence*, McGraw-Hill, New York, 1959.
- [2] R. D. Moser, J. Kim and N. N. Mansour, `http://turbulence.ices.utexas.edu/data/MKM/chan590`.
- [3] F. Nicoud and F. Ducros, *Subgrid-scale stress modelling based on the square of the velocity gradient tensor*, Flow, Turbulence and Combustion, 62:183-200,1999.
- [4] B. Mohammadi, O. Pironneau, P. G. Ciarlet and J.-L. Lions, *Analysis of the K-Epsilon turbulence model*, John Wiley & Sons - Masson, 1994.
- [5] R. B. Dean, *Reynolds Number Dependence of Skin Friction and Other Bulk Flow Variables in Two-Dimensional Rectangular Duct Flow*, Journal of Fluids Engineering, 100:215-223, 1978.
- [6] P.-E. Angeli, *Simulation numérique de la turbulence dans Trio_U : nouvelle méthode de prise en compte des lois de paroi via une condition aux limites de symétrie et un terme source de type Robin*, CEA Technical note, DEN_DANS_DM2S_STMF_LMSF_NT_13-011A, 2013.

2 Theoretical features

See the technical note [6] for detailed explanations.

• *Standard wall treatment approach in Trio_U*:

The wall laws for velocity and temperature used in the code can be written as $u_\tau = f(u_\tau)$ and $T_\tau = f(T_\tau)$. At each time step, a fixed point resolution of these equations gives respectively the values of u_τ and T_τ. Hence the velocity gradient and the temperature gradient at the wall are deduced. These gradients are used respectively in the momentum and energy balances for wall elements, were they replace the calculated gradients which are wrong due to the low resolution of the grid.

• *New approach validated here*:

The methodology is briefly described in [4] and is here referred to as the *Pironneau* approach. The idea is that the fixed walls are replaced by symetries, so that the velocity and temperature gradients appearing in the momentum and energy balances are zero. Formally, the gradients calculated from the wall laws are added then to these balances, instead of replacing wrong values like in the standard approach. Let y_1 be the distance from the wall of the first calculation point. The wall law results actually in a Robin boundary condition under the form $\left.\frac{\partial u}{\partial y}\right|_w = f[u(y_1)]$, which is implemented by a source term in the code. The same methodology is applied for temperature. More generally, the Robin condition can be evaluated at a distance δ from the wall: $\frac{\partial u}{\partial n}(\delta) = f[u(\delta)]$. Thus the user has to choose the value of δ, such that δ is located in the logarithmic layer. Here we choose $\delta = y_1$.

3 Tests description

The present calculations are L.E.S. of turbulence in a 3D biperiodic channel flow with $Re_\tau = 590$. The dimensions of the channel are: $L_x = 6.4$ m , $L_y = 2h = 2$ m, $L_z = 3.2$ m.

Two simulations using the standard methodology are first carried out (one using a VDF discretization and the other using a VEF discretization). Then two others simulations (in VEF) using the new approach are done. In the second one, the upper and lower walls of the channel are displaced from the distance δ toward the centerline of the channel, and a new mesh similar to the previous one is built.

3.1 VDF mesh

Number of nodes in each direction: $N_x = 55$, $N_y = 36$, $N_z = 34$.

Total number of elements: $(N_x\text{-}1)(N_y\text{-}1)(N_z\text{-}1) = 62370$.

$$dx^+ = \frac{L_x}{N_x - 1}\frac{\mathrm{Re}_\tau}{h} = 70 \; ; \; y^+ = \frac{L_y}{2(N_y - 1)}\frac{\mathrm{Re}_\tau}{h} = 17 \; ; \; dz^+ = \frac{L_z}{N_z - 1}\frac{\mathrm{Re}_\tau}{h} = 57.$$

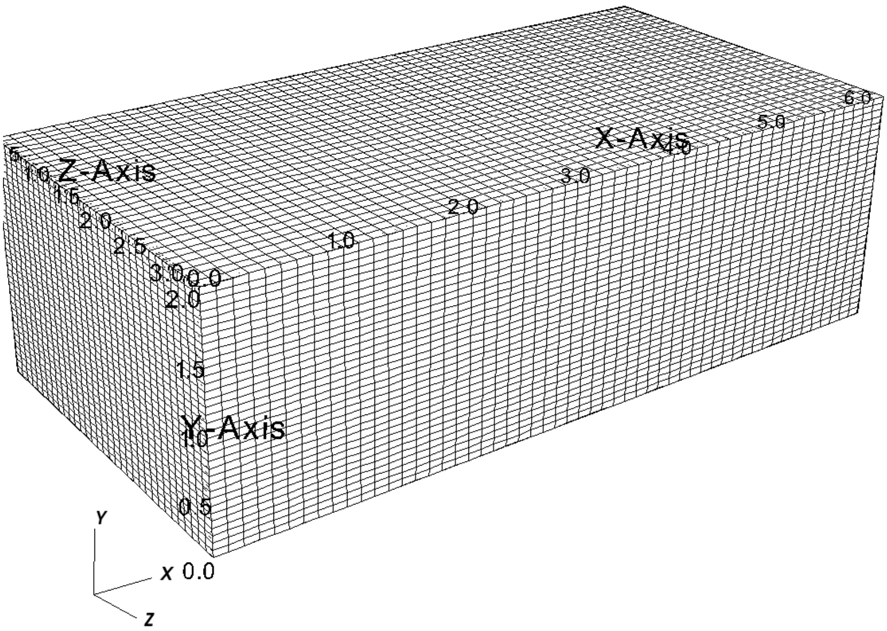

3.2 VEF mesh (entire channel)

Number of nodes in each direction: $N_x = 17$, $N_y = 11$, $N_z = 9$.

Total number of elements with `tetraedriser_homogene_fin`: $48(N_x\text{-}1)(N_y\text{-}1)(N_z\text{-}1) = 61440$.

$$dx^+ = \frac{L_x}{3(N_x - 1)}\frac{\mathrm{Re}_\tau}{h} = 79 \; ; \; y^+ = \frac{L_y}{6(N_y - 1)}\frac{\mathrm{Re}_\tau}{h} = 20 \; ; \; dz^+ = \frac{L_z}{3(N_z - 1)}\frac{\mathrm{Re}_\tau}{h} = 79.$$

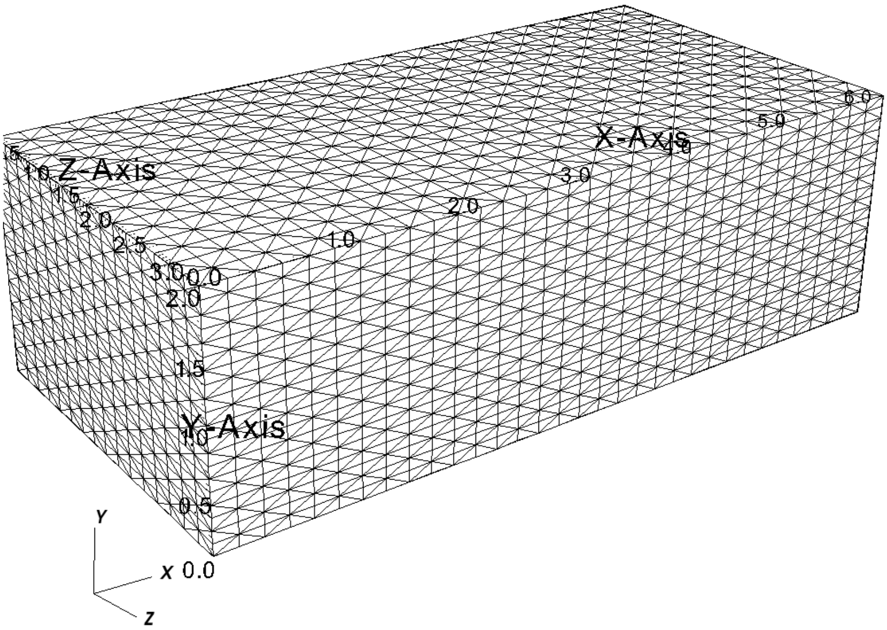

3.3 VEF mesh (truncated channel)

Number of nodes in each direction: $N_x = 17$, $N_y = 11$, $N_z = 9$.
Total number of elements with `tetraedriser_homogene_fin`: $48(N_x\text{-}1)(N_y\text{-}1)(N_z\text{-}1) = 61440$.

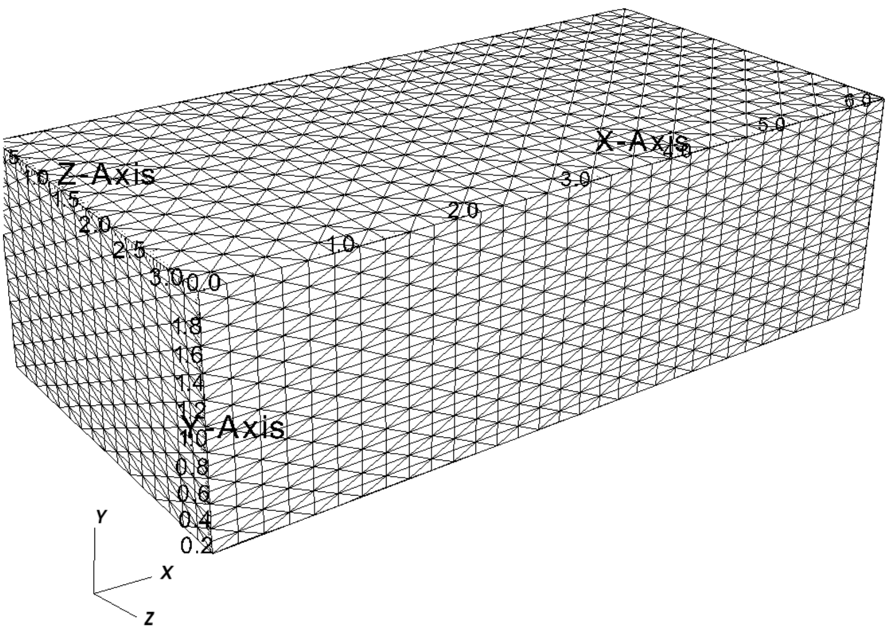

3.4 Physical properties and dimensionless numbers

Physical properties:

- $\rho = 0.011928 \text{ kg} \cdot \text{m}^{-3}$
- $\mu = 2.84\text{e-}5 \text{ kg} \cdot \text{m}^{-1} \cdot \text{s}^{-1}$

Dimensionless numbers:

- $\text{Re}_b = \dfrac{\rho U_b h}{\mu} = 10759$, where $U_b = \dfrac{2}{3} U_c$ and $U_c = 38.4264 \text{ m} \cdot \text{s}^{-1}$ (*cf.* initial condition)
- $\text{Re}_\tau = 0.175 \text{Re}_b^{7/8} = 590$ (Dean's correlation [5])

3.5 Initial and boundary conditions

Initial conditions:

- Parabolic mean profile for the x-component of velocity:
  `Champ_init_canal_sinal 3 { Ucent 38.4264 h 1 ampli_sin 0 omega 1 ampli_bruit 0.5 }`

Boundary conditions:

- Inlet/outlet (x-direction): periodicity
- Front/back boundaries (z-direction): periodicity
- Top/low boundaries:
  - `paroi_fixe` for the Trio_U "standard" approach
  - `paroi_decalee_Robin { _delta_value_ }` for the "Pironneau" approach$^{(*)}$

Source term in the "Pironneau" approach:

`source_Robin 2 Haut Bas`

$^{(*)}$ where `_delta_value_` is set according the recommandation of section 2 ($\delta = y_1$).

3.6 Numerical schemes

VDF discretization:

- Time scheme: third order Runge-Kutta method with `facsec`=1
- Convection: centered scheme

VEF discretization:

- Time scheme: third order Runge-Kutta method with `facsec`=1
- Convection: `EF_stab` with $\alpha = 0.2$

4 Friction velocity and friction Reynolds number calculated

4.1 Friction velocity u_τ

	time (s)	u_τ ($\text{m} \cdot \text{s}^{-1}$)	Relative error (%)
Theoretical $^{(*)}$	-	1.40476	-
VDF	50	1.39799	0.48
VEF	50	1.27989	8.89
VEF Pironneau	50	1.2424	11.56
VEF Pironneau (shifted mesh)	50	1.28183	8.75

(*) according to Dean's correlation [5]: $\mathrm{Re}_\tau = 0.175\mathrm{Re}_b^{7/8}$, and using $\mathrm{Re}_\tau = \dfrac{\rho u_\tau h}{\mu}$.

4.2 Friction Reynolds Re_τ

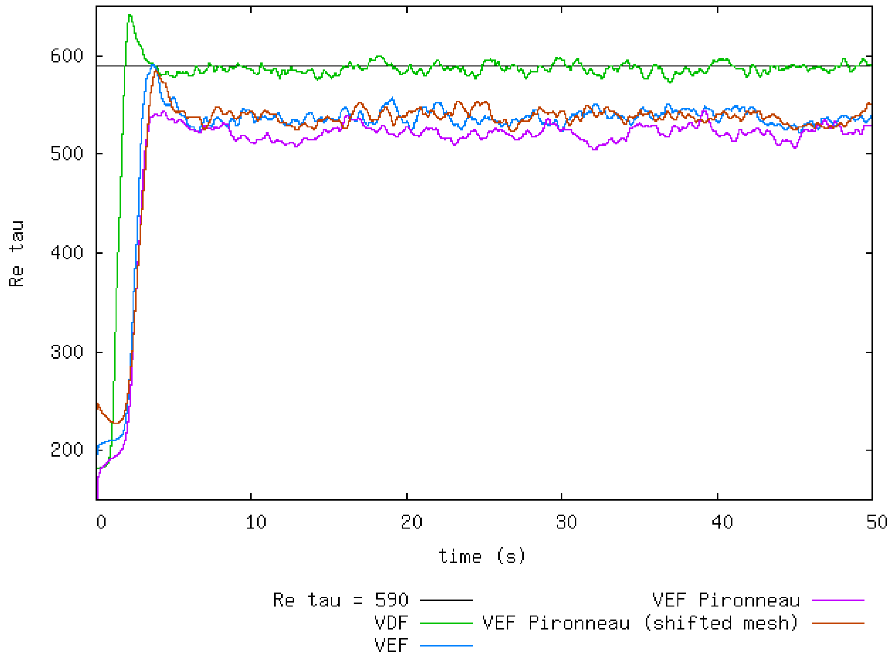

5 Detailed results

In the next two sections, different time- and space-averaged profiles are plotted across the channel half-height: the components of velocity (u and w), the components of the subscale stress tensors (T_{ij}), as well as the adimensional equivalent quantities.

We compare the non-dimensional mean velocity profiles with the Reichardt's law [1]:

$U^+ = \dfrac{1}{\kappa}\ln(1+\kappa y^+) + A\left(1 - e^{-y^+/11} - \dfrac{y^+}{11}e^{-y^+/3}\right)$, were $\kappa = 0.415$ and A = 7.44.

5.1 Mean x-velocity profile $< u >$

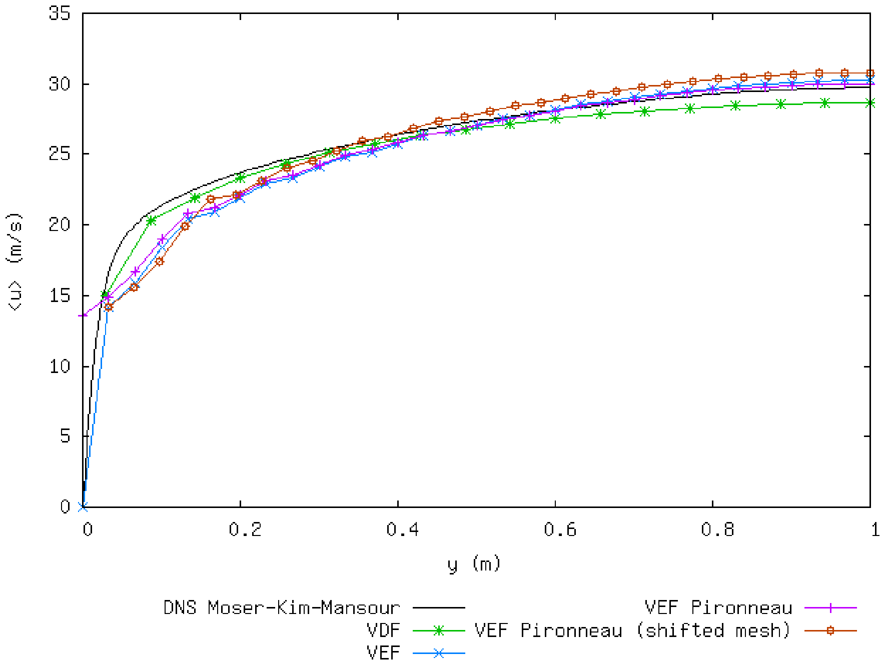

5.2 Non-dimensional mean x-velocity profile $< u^+ >$

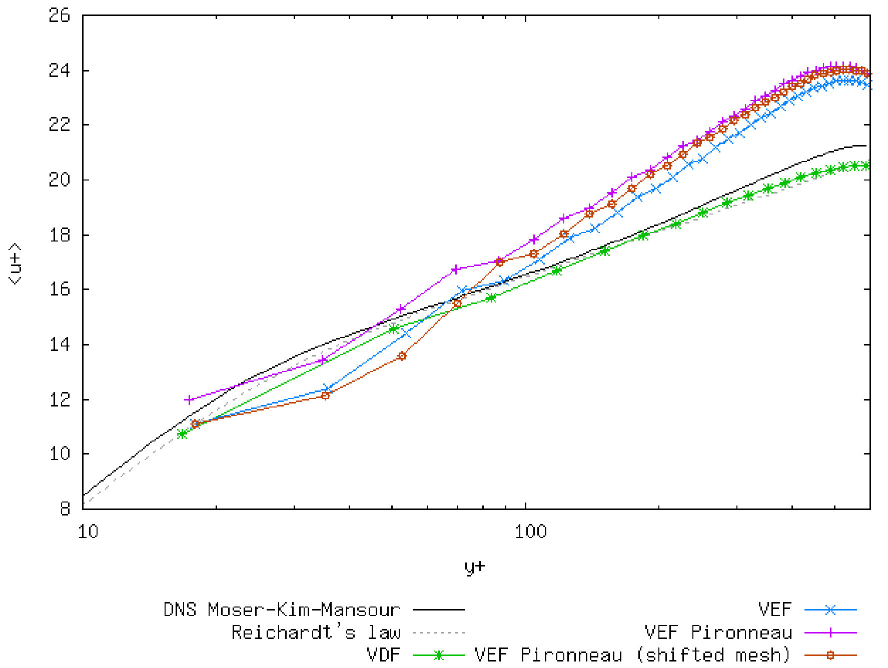

5.3 Mean z-velocity profile $< w >$

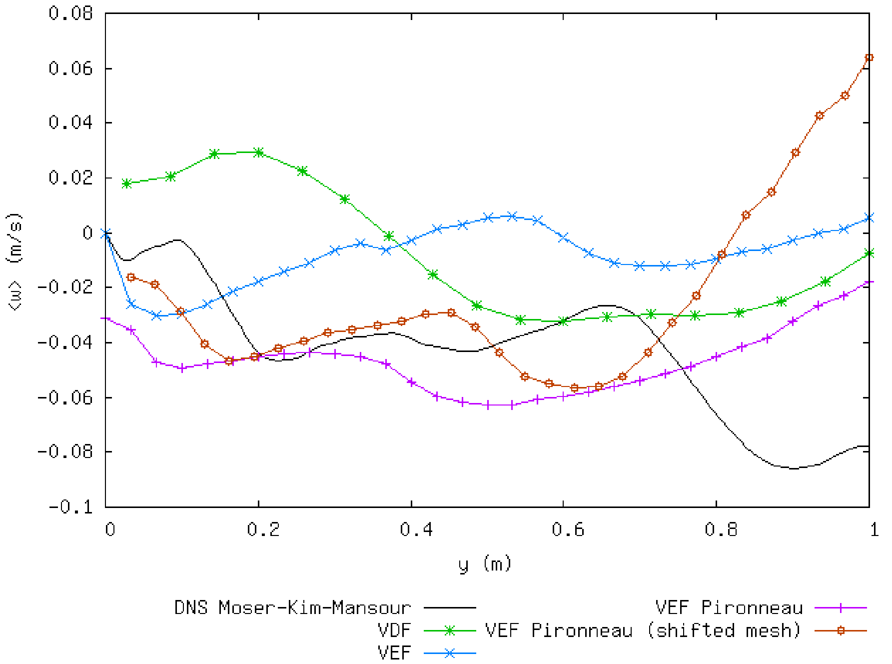

5.4 Non-dimensional mean z-velocity profile $< w^+ >$

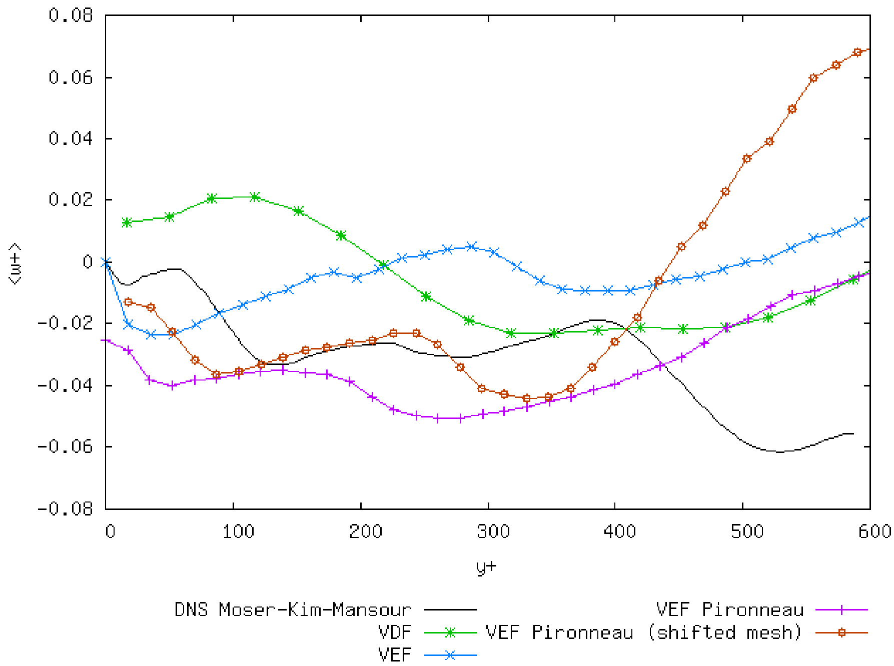

5.5 Mean xx-component of subgrid scale tensor $< T_{11} >$

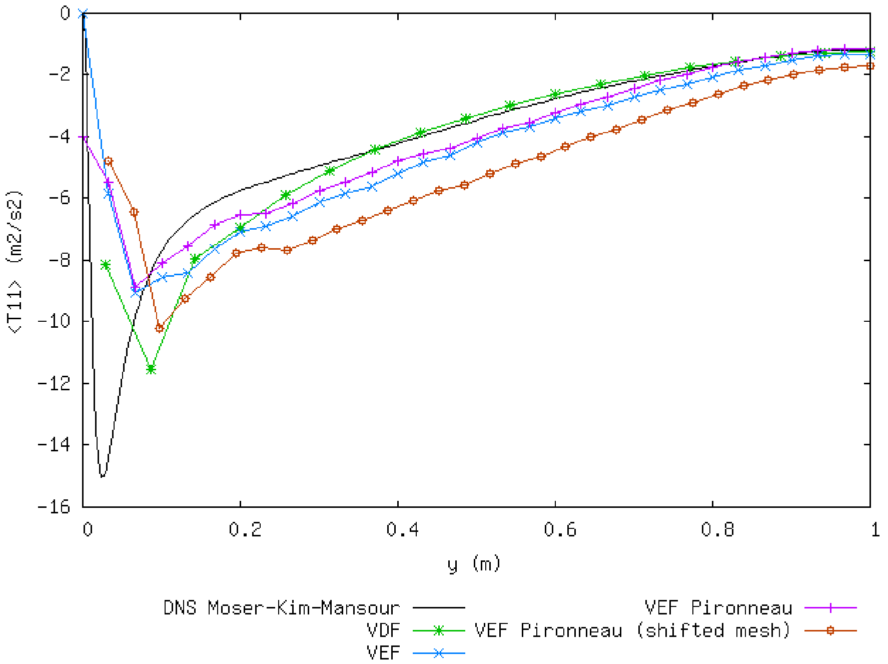

5.6 Non-dimensional mean xx-component of subgrid scale tensor $< T_{11}^{+} >$

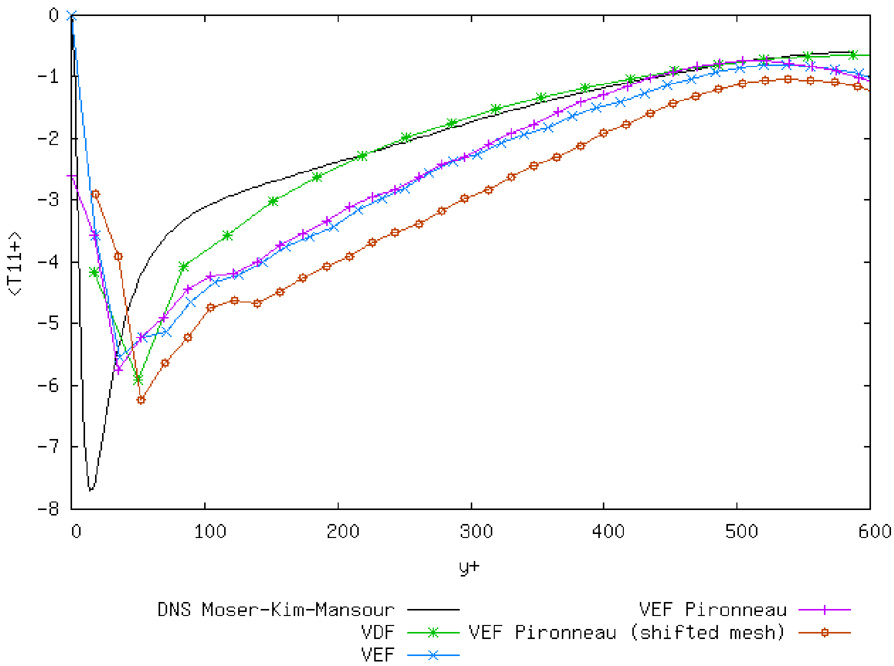

5.7 Mean yy-component of subgrid scale tensor $< T_{22} >$

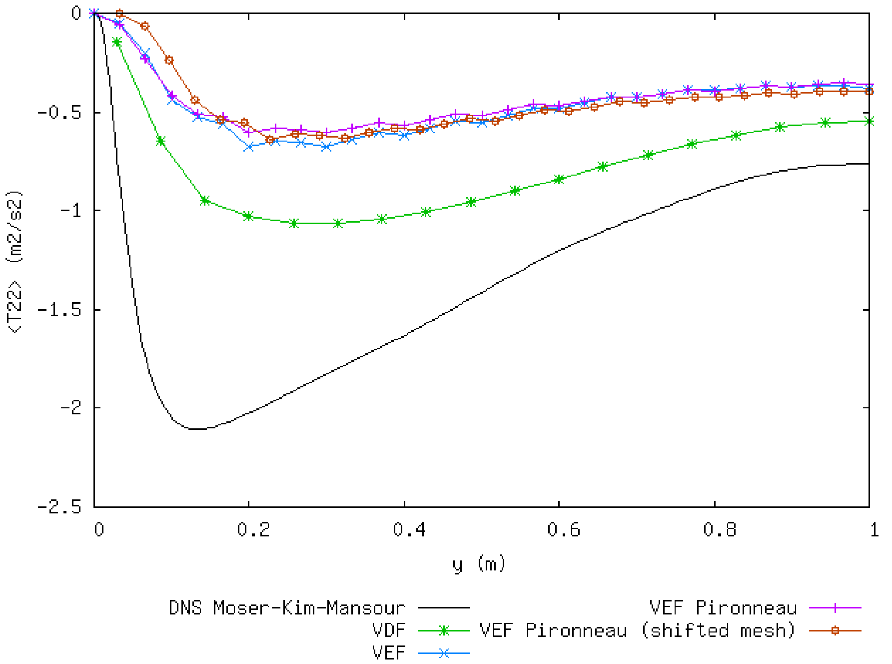

5.8 Non-dimensional mean yy-component of subgrid scale tensor $< T_{22}^{+} >$

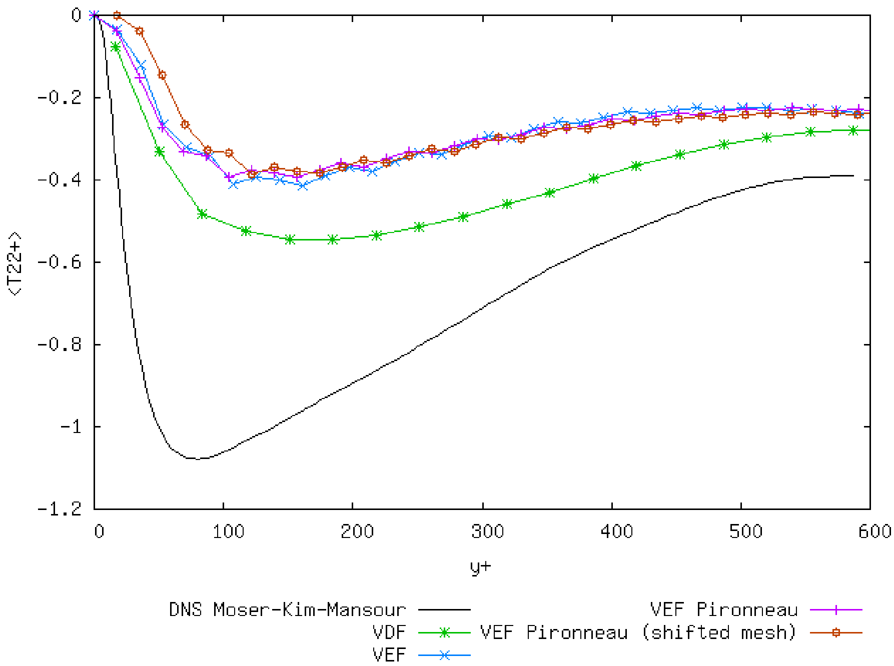

5.9 Mean zz-component of subgrid scale tensor $< T_{33} >$

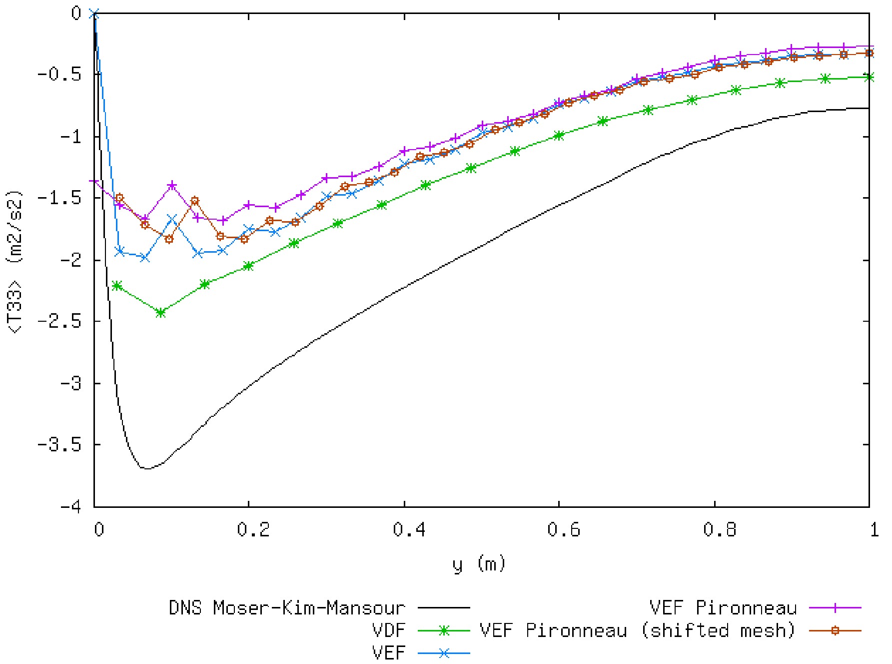

5.10 Non-dimensional mean zz-component of subgrid scale tensor $< T_{33}^{+} >$

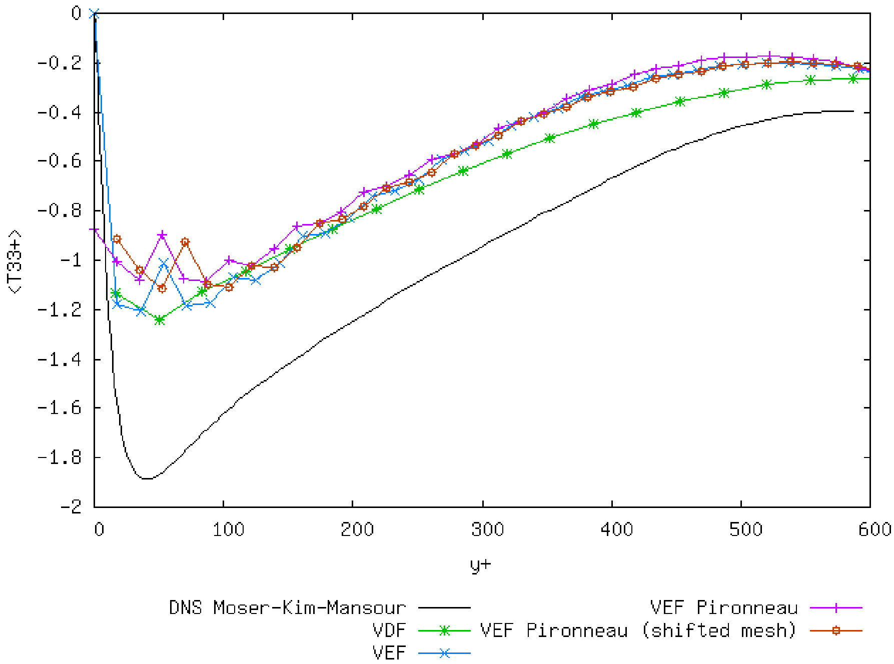

5.11 Mean xy-component of subgrid scale tensor $< T_{12} >$

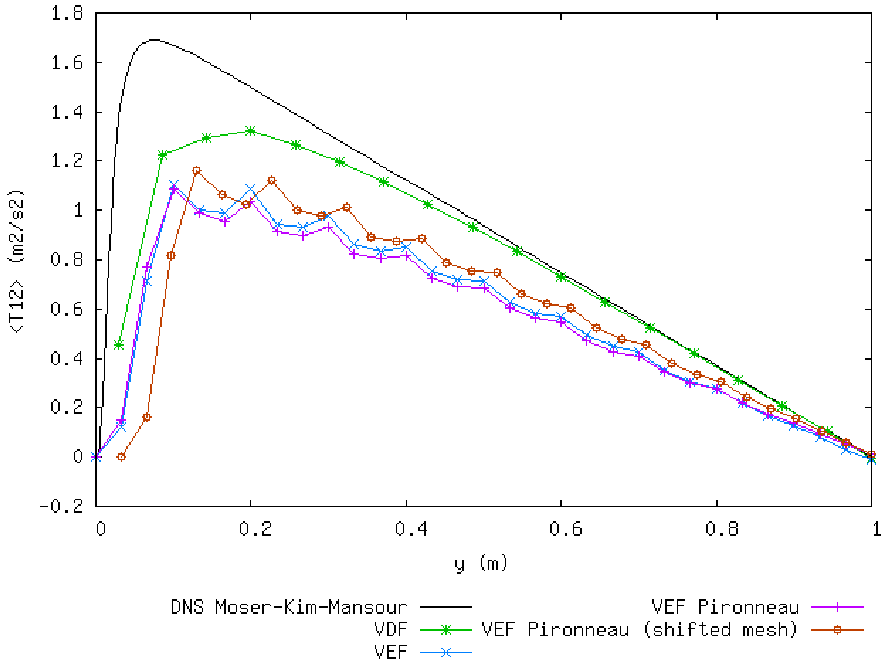

5.12 Non-dimensional mean xy-component of subgrid scale tensor $< T_{12}^{+} >$

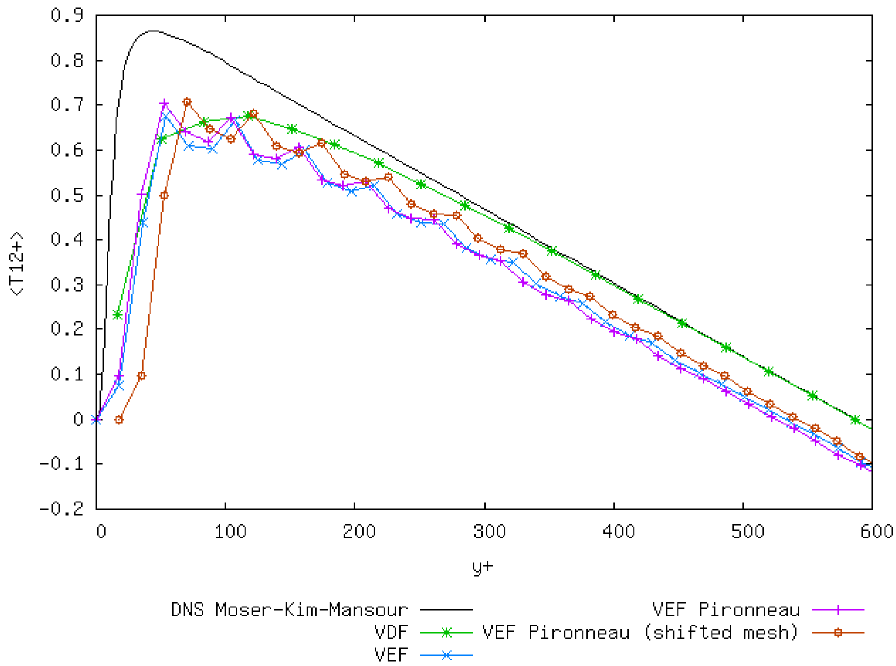

5.13 Mean xz-component of subgrid scale tensor $< T_{13} >$

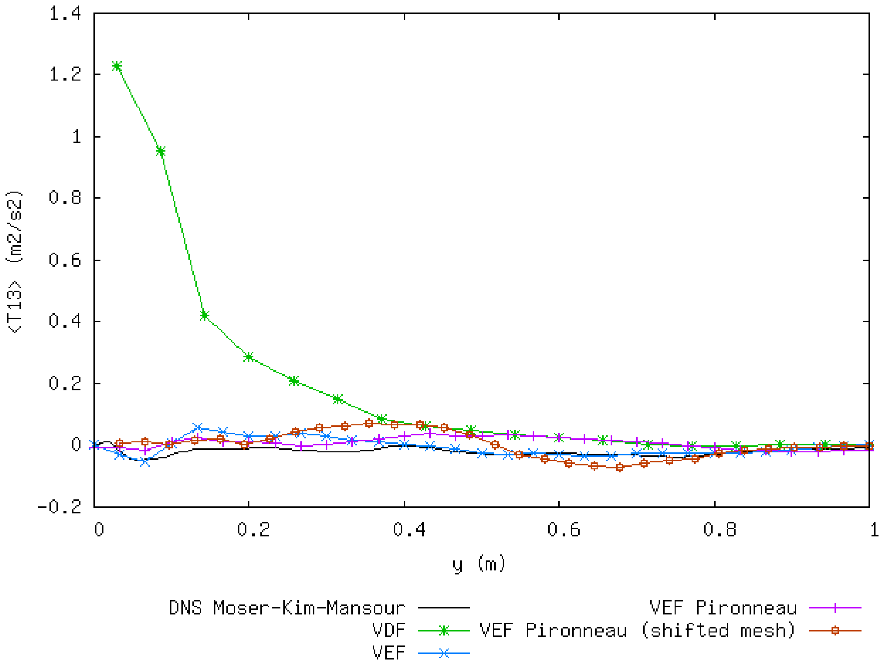

5.14 Non-dimensional mean xz-component of subgrid scale tensor $< T_{13}^{+} >$

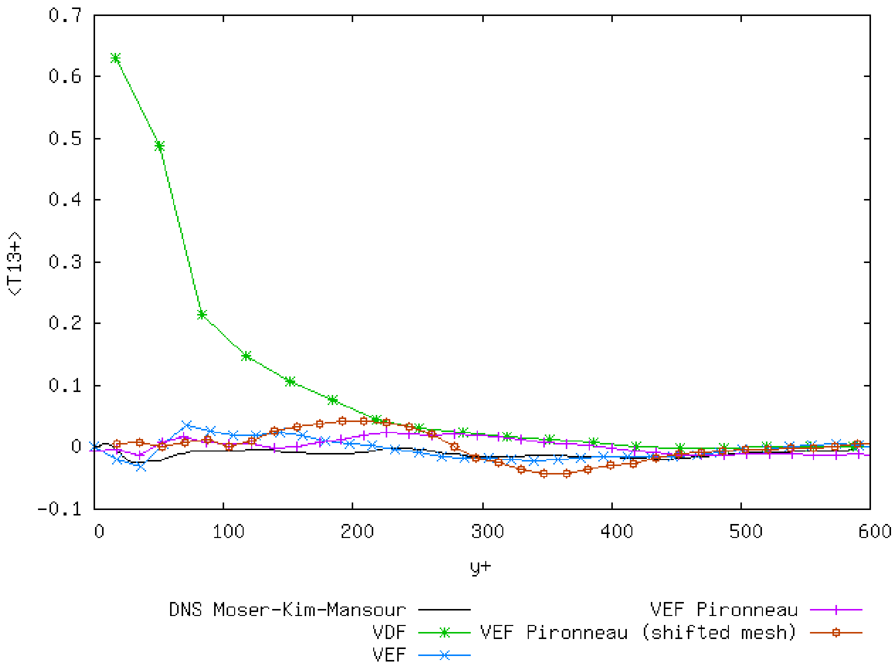

5.15 Mean yz-component of subgrid scale tensor $< T_{23} >$

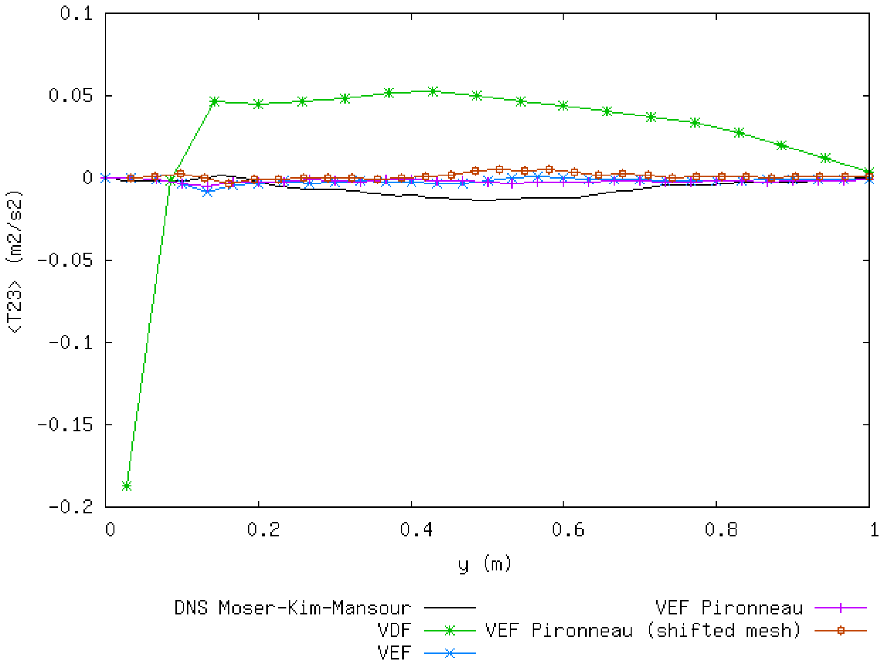

5.16 Non-dimensional mean yz-component of subgrid scale tensor $< T_{23}^{+} >$

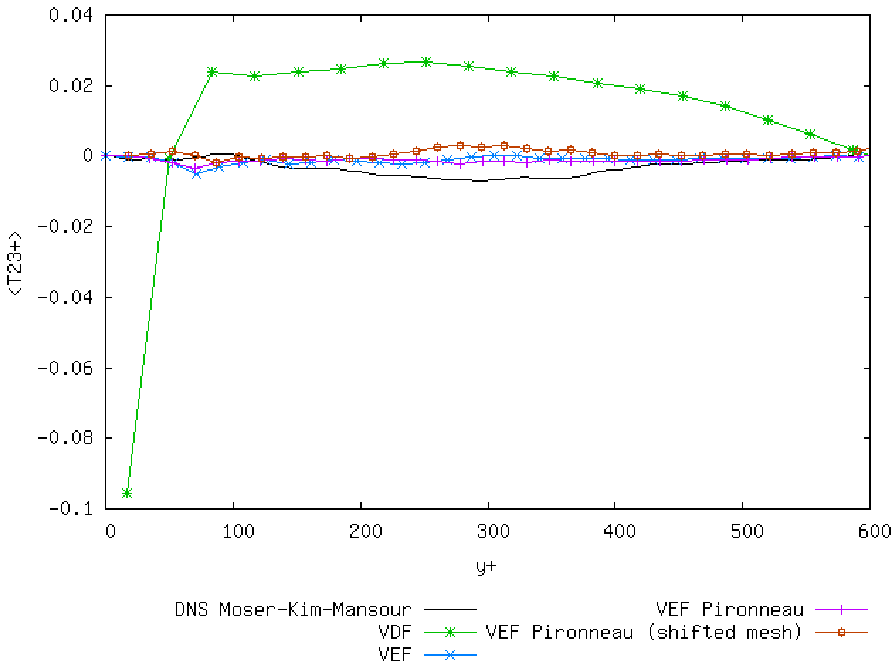

6 Analysis of the results

- On the whole, the VDF simulation seems to give better results than the VEF simulations. The VEF simulations (standard and new approachs) are relatively similar.
- Friction velocity: the best friction velocity in the comparison with the theoretical value is obtained with the VDF simulation. The Pironneau simulations give similar relative errors than the standard approach, but the truncated channel is slightly better whereas the whole channel is not as good than the non-Pironneau simulation. The truncated channel with the Pironneau approach gives the same relative error than the simulation using the former approach.
- For the non-dimensional mean x-velocity profile $< u >$, the first calculation points for all simulations are located on the Reichardt's law as expected, except for the VEF Pironneau. In this case, the real first point is not represented on the logarithmic graph because it corresponds to $y = 0$. Thus the first represented point of the VEF Pironneau profile (in fact the second calculated point) has no reason to satisfy the Reichardt's law.
- Subscale stress tensor components $< T_{ij} >$: the tendancies are in correct agreement with the DNS results of Moser-Kim-Mansour, except the VDF simulation which gives bad results on particular components.

7 Computer performance

	host	system	Total CPU Time	CPU time/step	number of cell
T0Q_VDF/Cas	vonnes	Linux	11002.3	0.526339	62370
T0Q_VEF/Cas	vonnes	Linux	114358	1.44713	61440
T0Q_VEF_Pironneau/Cas	vonnes	Linux	99892	1.30007	61440
T0Q_VEF_Pironneau_maillage_decale/Cas	vonnes	Linux	104195	1.2958	61440
Total			329447		

8 Data Files

8.1 Cas

```
Dimension 3
Pb_Hydraulique_Turbulent pb
Domaine dom
Mailler dom
{
  Pave Cavite
  {
    Origine 0 0 0
    Nombre_de_Noeuds 17 11 9
    Longueurs 6.4 2 3.2
    Facteurs 1 1 1
  }
  {
    Bord PerioX X = 0    0 <= Y <= 2 0 <= Z <= 3.2
    Bord PerioX X = 6.4    0 <= Y <= 2 0 <= Z <= 3.2
    Bord PerioZ Z = 0    0 <= X <= 6.4       0 <= Y <= 2
    Bord PerioZ Z = 3.2    0 <= X <= 6.4       0 <= Y <= 2
    Bord Bas   Y = 0 0 <= X <= 6.4      0 <= Z <= 3.2
    Bord Haut Y = 2 0 <= X <= 6.4      0 <= Z <= 3.2
  }
}
Tetraedriser_homogene_fin dom
Reordonner_faces_periodiques dom PerioX
Reordonner_faces_periodiques dom PerioZ
VEFPreP1b dis
Runge_Kutta_ordre_3 sch_RK3
Lire sch_RK3
{
  tinit 0
  tmax 50
  dt_start dt_calc
  dt_min 1e-7
  dt_max 1
  dt_impr 1
  dt_sauv 25
  seuil_statio 1e-15
  facsec 1
  no_check_disk_space
  periode_sauvegarde_securite_en_heures 11
}
Fluide_incompressible air
Lire air
{
  mu  champ_uniforme 1 2.84e-5
  rho champ_uniforme 1 0.011928
}
Champ_uniforme gravite
Lire gravite 3 0 0 0
Associer air gravite
Associer pb dom
```

```
Associer pb sch_RK3
Associer pb air
Discretiser pb dis
Lire pb
{
  Navier_Stokes_turbulent
  {
    Solveur_pression  petsc Cholesky { }
    Convection    { EF_stab { volumes_etendus alpha 0.2 } }
    Diffusion   { }
    Conditions_initiales  { vitesse champ_init_canal_sinal 3 { Ucent 38.4264 h 1 ampli_sin 0 on
    Conditions_limites  {
          PerioX  periodique
          PerioZ  periodique
          Haut  paroi_fixe
          Bas paroi_fixe
          }
    Modele_turbulence sous_maille_WALE
          {
          turbulence_paroi loi_standard_hydr
          dt_impr_ustar 1
          }
    Traitement_particulier  {
          canal {
            dt_impr_moy_spat 10
            dt_impr_moy_temp 10
            debut_stat 20
            }
          }
    Sources     { canal_perio { direction_ecoulement 0 } }
  }
  Postraitement
  {
  Definition_champs   {
          moyenne_vitesse   Moyenne { t_deb 20 t_fin 50 source refChamp { Pb_champ pb vitesse }
          ecart_type_vitesse  Ecart_type { t_deb 20 t_fin 50 source refChamp { Pb_champ pb vite
          }
    Sondes      {
          sonde_vitesse     nodes vitesse     periode 0.05 points 1 3.2 1 1.6
          sonde_moyenne_vitesse   nodes moyenne_vitesse   periode 0.05 points 1 3.2 1 1.6
          sonde_ecart_type_vitesse  nodes ecart_type_vitesse  periode 0.05 points 1 3.2 1 1.6
          coupe_vitesse     nodes vitesse     periode 0.5 segment 21 0.066667 0 0.066667  0.066
          coupe_moyenne_vitesse   nodes moyenne_vitesse   periode 0.5 segment 21 0.066667 0 0.0
          coupe_ecart_type_vitesse  nodes ecart_type_vitesse  periode 0.5 segment 21 0.066667 0
          }
    Format lata_v2
    Champs dt_post 10 {
          vitesse som
          }
    Statistiques dt_post 10
          {
          t_deb 20 t_fin 50
          moyenne vitesse
          ecart_type vitesse
```

```
        }
    }
    sauvegarde formatte pb.sauv
}
Resoudre pb
Fin
```

8.2 Cas

```
Dimension 3
Pb_Hydraulique_Turbulent pb
Domaine dom
Mailler dom
{
    Pave Cavite
    {
        Origine 0 0 0
        Nombre_de_Noeuds 17 11 9
        Longueurs 6.4 2 3.2
        Facteurs 1 1 1
    }
    {
        Bord PerioX X = 0    0 <= Y <= 2 0 <= Z <= 3.2
        Bord PerioX X = 6.4    0 <= Y <= 2 0 <= Z <= 3.2
        Bord PerioZ Z = 0    0 <= X <= 6.4      0 <= Y <= 2
        Bord PerioZ Z = 3.2    0 <= X <= 6.4      0 <= Y <= 2
        Bord Bas   Y = 0 0 <= X <= 6.4      0 <= Z <= 3.2
        Bord Haut Y = 2 0 <= X <= 6.4      0 <= Z <= 3.2
    }
}
Tetraedriser_homogene_fin dom
Reordonner_faces_periodiques dom PerioX
Reordonner_faces_periodiques dom PerioZ
VEFPreP1b dis
Runge_Kutta_ordre_3 sch_RK3
Lire sch_RK3
{
    tinit 0
    tmax 50
    dt_start dt_calc
    dt_min 1e-7
    dt_max 1
    dt_impr 1
    dt_sauv 25
    seuil_statio 1e-15
    facsec 1
    no_check_disk_space
    periode_sauvegarde_securite_en_heures 11
}
Fluide_incompressible air
Lire air
{
    mu  champ_uniforme 1 2.84e-5
    rho champ_uniforme 1 0.011928
```

```
}
Champ_uniforme gravite
Lire gravite 3 0 0 0
Associer air gravite
Associer pb dom
Associer pb sch_RK3
Associer pb air
Discretiser pb dis
Lire pb
{
  Navier_Stokes_turbulent
  {
    Solveur_pression   petsc Cholesky { }
    Convection     { EF_stab { volumes_etendus alpha 0.2 } }
    Diffusion   { }
    Conditions_initiales  { vitesse champ_init_canal_sinal 3 { Ucent 38.4264 h 1 ampli_sin 0 on
    Conditions_limites  {
          PerioX  periodique
          PerioZ  periodique
          Haut  paroi_decalee_Robin { delta 0.033333 }
          Bas paroi_decalee_Robin { delta 0.033333 }
          }
    Modele_turbulence sous_maille_WALE
          {
          turbulence_paroi loi_standard_hydr
          dt_impr_ustar 1
          }
    Traitement_particulier  {
          canal {
            dt_impr_moy_spat 10
            dt_impr_moy_temp 10
            debut_stat 20
            }
          }
    Sources     { canal_perio { direction_ecoulement 0 } }
    Sources     { source_Robin 2 Haut Bas 0.0005 }
  }
  Postraitement
  {
  Definition_champs   {
          moyenne_vitesse   Moyenne { t_deb 20 t_fin 50 source refChamp { Pb_champ pb vitesse }
          ecart_type_vitesse  Ecart_type { t_deb 20 t_fin 50 source refChamp { Pb_champ pb vite
          }
    Sondes      {
          sonde_vitesse     nodes vitesse     periode 0.05 points 1 3.2 1 1.6
          sonde_moyenne_vitesse   nodes moyenne_vitesse   periode 0.05 points 1 3.2 1 1.6
          sonde_ecart_type_vitesse  nodes ecart_type_vitesse  periode 0.05 points 1 3.2 1 1.6
          coupe_vitesse     nodes vitesse     periode 0.5 segment 21 0.066667 0 0.066667  0.066
          coupe_moyenne_vitesse   nodes moyenne_vitesse   periode 0.5 segment 21 0.066667 0 0.0
          coupe_ecart_type_vitesse  nodes ecart_type_vitesse  periode 0.5 segment 21 0.066667 0
          }
    Format lata_v2
    Champs dt_post 10 {
          vitesse som
```

```
          }
    Statistiques dt_post 10
          {
          t_deb 20 t_fin 50
          moyenne vitesse
          ecart_type vitesse
          }
  }
  sauvegarde formatte pb.sauv
}
Resoudre pb
Fin
```